Kinetic and Thermodynamic Studies of the Reactivity of (Trimethylsilyl)diazomethane with $HMo(CO)_3(C_5R_5)$ (R = H, Me). Estimation of the Mo−$N_2CH_2SiMe_3$ Bond Strength and Experimental Determination of the Enthalpy of Formation of (Trimethylsilyl)diazomethane

George C. Fortman,[†] Derek Isrow,[†] James E. McDonough,[†] Paul von Ragué Schleyer,*[,‡] Henry F. Schaefer III,*[,‡] Brian Scott,[§] Gregory J. Kubas,*[,§] Tamás Kégl,*[,||] Ferenc Ungváry,*[,||] and Carl D. Hoff*[,†]

Department of Chemistry, University of Miami, Coral Gables, Florida, 33126, Department of Chemistry and Center for Computational Chemistry, University of Georgia, Athens, Georgia 30606, Structural Inorganic Chemistry Group, Chemistry Division, MS J514, Los Alamos National Laboratory, Los Alamos, New Mexico, 87545, and Department of Organic Chemistry, University of Pannonia, Veszprém, H-8201, Hungary

Received April 15, 2008

The rates of reaction of $N_2CHSiMe_3$ with $HMo(CO)_3Cp$ ($Cp = \eta^5$-C_5H_5) in heptane obey the rate law $-d[HMo(CO)_3Cp]/dt = k[HMo(CO)_3Cp][N_2CHSiMe_3]$ ($k = 0.035 \pm 0.01$ M^{-1} s^{-1} at 0 °C; $\Delta H^{\ddagger} = 11.7 \pm 2.0$ kcal/mol and $\Delta S^{\ddagger} = -22.0 \pm 3.0$ cal/(mol K)). Isotopic scrambling between $DMo(CO)_3Cp$ and $N_2CHSiMe_3$ occurs at a rate faster than the overall reaction. Reversible 1,2-addition to form the tightly bound intermediate $[Me_3SiCH_2N_\beta{=}N_\alpha{}^{\delta+}][{}^{\delta-}Mo(CO)_3Cp]$ is proposed as the first step of the reaction. Spectroscopic and computational data support this formulation. The contact ion pairs can undergo heterolytic cleavage to ions or homolytic cleavage to radicals, and the solvent influence on k_{obs} (THF > toluene > heptane) is interpreted in terms of this model. The enthalpy of this reaction has been measured by solution calorimetry at 272 K in THF: $\Delta H = -11.6 \pm 1.2$ kcal/mol. These data, together with computed organic reaction energies allow estimation of the bond strength between the three-electron donors $\cdot N_2CHSiMe_3$ and $\cdot Mo(CO)_2Cp$ to be 25 ± 5 kcal/mol stronger than the two-electron Mo−CO bond. Coordination of $N_2CHSiMe_3$ to the complexes $M(PR_3)_2(CO)_3$ (M = Mo, W; R = Cy, ^{i}Pr; Cy = cyclohexyl; ^{i}Pr = isopropyl) alters the course of reaction with $HMo(CO)_3Cp$. The stoichiometric reaction of $Me_3SiCH{=}N{=}NMo(P^iPr_3)_2(CO)_3$ with 2 equiv of $HMo(CO)_3Cp$ produces $SiMe_4$, $Mo(N_2)(P^iPr_3)_2(CO)_3$, and $[Mo(CO)_3Cp]_2$. In the presence of excess $N_2CHSiMe_3$ this reaction is catalytic and has been used to experimentally measure the heat of hydrogenation of $N_2CHSiMe_3$ to N_2 and $SiMe_4$ by 2 equiv of $HMo(CO)_3Cp$. The derived enthalpy of formation of $N_2CHSiMe_3$ (5.8 ± 3.0 kcal/mol) is in reasonable agreement with high-level theoretical calculations. X-ray crystal structure data are reported for $W(CO)_2(N_2CH_2SiMe_3)Cp$: triclinic, space group $P\bar{1}$, $a = 6.3928(7)$ Å, $b = 10.6551(12)$ Å, $c = 10.8766(12)$ Å, $\alpha = 100.632(2)°$, $\beta = 96.254(2)°$, $V = 721.32$ Å^3, $Z = 2$.

Introduction

The first transition-metal complex containing a bound diazo group was prepared according to eq 1 by Bisnette and King more than 40 years ago.[1]

$$NaMo(CO)_3Cp + [ArN_2]^+[BF_4]^- \rightarrow Mo(CO)_2(N_2Ar)Cp + CO + NaBF_4 \quad (1)$$

At that time the authors noted that the relationship between $Mo(CO)_2(NO)Cp$ and $Mo(p\text{-}N_2C_6H_4OCH_3)(CO)_2Cp$ ($Cp = \eta^5$-C_5H_5) "appears to be especially close." This statement first highlighted the similarity of the $^{\bullet}NO$ and $^{\bullet}NNR$ ligands' binding properties to metal complexes. Quantitative estimates of the bond strength between metal centers and the three-electron donor $^{\bullet}NNR$ have not been reported. In fact, there are relatively few reports for the enthalpy of binding of $^{\bullet}NO$ to metal complexes. The enthalpies of the reactions shown in eqs 2 and 3 have been measured and yield estimates[2] of the Cr−NO and Mo−NO bond strengths at 70 and 83 kcal/mol, respectively.

$$^{\bullet}Cr(CO)_3Cp^* + {}^{\bullet}NO \rightarrow Cr(CO)_2(NO)Cp^* + (CO) \quad (2)$$

$$Mo([^tBu]Ar)_3 + {}^{\bullet}NO \rightarrow Mo(NO)(N[^tBu]Ar)_3 \quad (3)$$

These data show the high strength of the formal three-electron bond between a metal and $^{\bullet}NO$. Comparison of bond strengths between $^{\bullet}NO$ and $^{\bullet}NNR$ with metal complexes is of relevance to the conversion of dinitrogen to amines, since a possible first step in any such scheme may be formation of $L_nM{-}NNR$.

Unfortunately $^{\bullet}N{\equiv}NR$ is unstable with respect to loss of $^{\bullet}R$, and thus direct calorimetric measurements such as those made with $^{\bullet}N{\equiv}O$ cannot be made. To circumvent this problem, the

[†] University of Miami.
[‡] University of Georgia.
[§] Los Alamos National Laboratory.
[||] University of Pannonia.

(1) King, R. B.; Bisnette, M. B. *J. Am. Chem. Soc.* **1964**, *86*, 5694.

10.1021/om800336p CCC: $40.75
Publication on Web 09/06/2008

reaction of metal hydrides with diazoalkanes could be used to evaluate the thermochemistry of the formal insertion of N_2 into the Mo−R bond to form a metal diazo complex, provided the reaction is sufficiently clean to allow for a thermochemical study.

Herrmann[3] reported that $HW(CO)_3Cp$ reacts with diazomethane to produce the diazo complex shown in eq 4 as the major reaction product.

$$HW(CO)_3Cp + N_2CH_2 \rightarrow W(CO)_2(N_2CH_3)Cp + CO \quad (4)$$

A minor reaction pathway, however, produced a metal alkyl as shown in eq 5.

$$HW(CO)_3Cp + N_2CH_2 \rightarrow W(CO)_3(CH_3)Cp + N_2 \quad (5)$$

If conditions could be found such that the enthalpy of eq 4 could be measured, it would provide, in principle, an inroad to estimating the strength of the W−($NNCH_3$) bond in $W(CO)_2(N_2CH_3)Cp$. Furthermore, the difference between eqs 4 and 5 results in the reaction shown in eq 6.

$$W(CO)_3(CH_3)Cp + N_2 \rightarrow W(CO)_2(N_2CH_3)Cp + CO \quad (6)$$

This reaction corresponds to the formal insertion of N_2 into the metal−alkyl bond to form a diazenido complex, which is also accompanied by the elimination of CO. The energetics of reactions such as that shown in eq 6 are of clear relevance to catalytic and photochemical attempts to incorporate N_2 into the production of organic amines or other organonitrogen compounds.

Analysis of the CO insertion reaction was reported earlier[4] utilizing the thermochemical cycle shown in eq 7: The enthalpy

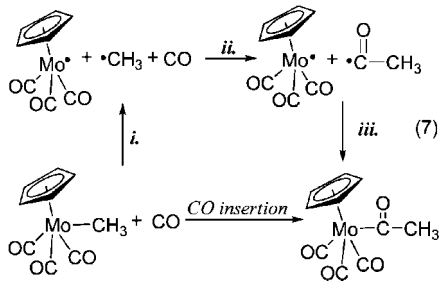

(7)

of carbonyl insertion was dominated by the organic radical addition (step 7-ii), which is exothermic by ∼12 kcal/mol and corresponds closely to the observed net enthalpy of reaction. The M−C bond strengths for the alkyl and acyl derivates (steps 7-i and 7-iii) roughly cancel. A corresponding scheme for analysis of N_2 insertion is shown in eq 8: In spite of the isoelectronic nature of CO and N_2, both the energetics and the structures of the products are different for these two cycles. Formation of the acyl radical $^{\bullet}C(=O)CH_3$ is exothermic, and its stability can be experimentally determined. Diazenido radicals such as $^{\bullet}NNCH_3$ are unstable and are best analyzed computationally. Another salient difference between eqs 7 and 8 is that the enthalpies of steps 7-i and 7-iii were found to largely cancel while the same cannot be expected for steps 8-i and 8-iii.

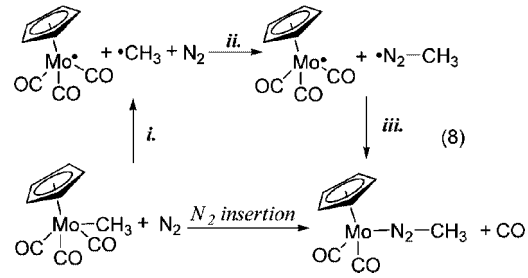

(8)

One other obstacle in the task of evaluating the thermochemistry of organometallic diazo complexes is the uncertainty in experimental data on the enthalpy of formation of diazomethane itself. Recent computational results[5] suggest an enthalpy of formation of ∼65 kcal/mol for CH_2N_2(g). This is considerably different than existing experimental[6] data of ∼50 kcal/mol.

For practical organometallic chemistry $N_2CHSiMe_3$ provides a useful starting material and an alternative to the more hazardous diazomethane. On the basis of the process pioneered by Seyferth and co-workers,[7] heptane solutions of $N_2CHSiMe_3$ are commercially available and stable for long periods of time. Reactions analogous to that shown in eq 4 were originally reported by Lappert[8] for the trimethylsilyl derivative. A stable $N_2CHSiMe_3$ adduct of Co(I) was recently reported by Caulton and co-workers,[9] while the structure and reactions of $Cp^*_2Ti(\eta^2$-$N_2CHSiMe_3)$ ($Cp^* = C_5Me_5$) were investigated by Bergman and co-workers.[10] The catalytic conversion of (trimethylsilyl)-diazomethane to the corresponding ketene by dicobalt octacarbonyl was recently reported,[11] as well as a mechanistic study of the reaction of $N_2CHSiMe_3$ with $^{\bullet}Cr(CO)_3C_5R_5$ ($R = H$, CH_3).[12]

This paper reports thermodynamic, kinetic, and computational data for the reaction of $HMo(CO)_3Cp$ (HMp) with $N_2CHSiMe_3$ to yield $Mo(CO)_2(N_2CH_2SiMe)_3Cp$ and CO. Also reported is a catalytic reaction in which $N_2CHSiMe_3$ is coordinated to $M(CO)_3(PR_3)_2$ ($M = Mo, W$; $R = Cy, {}^iPr$) and subsequently reacts with 2 equiv of $HMo(CO)_3Cp$. The bound diazo ligand is hydrogenated to form molecular nitrogen and TMS (TMS = $Si(CH_3)_4$), while the molybdenum hydride compound is converted to the dimer $[Mo(CO)_3Cp]_2$ (Mp_2). In addition to probes of the mechanisms of these reactions, reaction energetics relative to the insertion of dinitrogen into the metal−alkyl bond are investigated from both theoretical and experimental vantages. Finally, crystallographic structure data are reported for the complex $W(CO)_2(N_2CH_2SiMe_3)Cp$.

Results

Kinetics of the Reaction of $N_2CHSiMe_3$ with $HM(CO)_3(C_5R_5)$ ($M = Mo,W$; $R = H, CH_3$). Reaction of HMp with excess $N_2CHSiMe_3$ results in complete consumption of metal

(2) (a) Capps, K. B.; Bauer, A.; Sukcharoenphon, K.; Hoff, C. D. *Inorg. Chem.* **1999**, *38*, 6206. (b) Johnson, A. R.; Baraldo, L. M.; Cherry, J. P. F.; Tsai, Y. C.; Cummins, C. C.; Kryatov, S. V.; Rybak Akimova, V.; Capps, K. B.; Hoff, C. D.; Haar, C. M.; Nolan, S. P. *J. Am. Chem. Soc.* **2001**, *123*, 7271.

(3) Herrmann, W. A. *Angew. Chem.* **1975**, *87*, 358; *Angew. Chem., Int. Ed. Engl.* **1975**, *14*, 355.

(4) Nolan, S. P.; Lopez de la Vega, R.; Mukerjee, S. K.; Hoff, C. D. *Inorg. Chem.* **1986**, *25*, 1160.

(5) Dixon, D. A.; de Jong, W. A.; Peterson, K. A.; McMahon, T. B. *J. Phys. Chem. A.* **2005**, *109*, 4073.

(6) (a) http://webbook.nist.gov. (b) Foster, M. S.; Beauchamp, J. L. *J. Am. Chem. Soc.* **1972**, *94*, 2425. (c) Hassler, J. C.; Setser, D. W. *J. Am. Chem. Soc.* **1965**, *87*, 3793.

(7) Seyferth, D.; Dow, A. W.; Menzel, H.; Flood, T. C. *J. Am. Chem. Soc.* **1968**, *90*, 1080.

(8) Lappert, M. F.; Poland, J. S. *Chem. Commun.* **1969**, 1061.

(9) Ingleson, M. J.; Pink, M.; Caulton, K. G. *J. Am. Chem. Soc.* **2006**, *128*, 4248.

(10) Polse, J. L.; Kaplan, A. W.; Andersen, R. A.; Bergman, R. G. *J. Am. Chem. Soc.* **1998**, *120*, 6316.

(11) (a) Ungvári, N.; Kegl, T.; Ungváry, F. *J. Mol. Catal. A* **2004**, *219*, 7. (b) Tuba, R.; Ungvary, F. *J. Mol. Catal. A* **2003**, *203*, 59.

(12) Fortman, G. C.; Kegl, T.; Li, Q.-S.; Zhang, X.; Schaefer, H. F., III; Xie, Y.; King, R. B.; Telser, J.; Hoff, C. D. *J. Am. Chem. Soc.* **2007**, *129*, 14388.

Table 1. Relative Product Distribution Based on Solvent for the Reaction of $HMo(CO)_3Cp$ with $N_2CHSiMe_3$

	product distribn (%)		
solvent	Mo−$N_2CH_2SiMe_3$[a]	Mp-CH_2SiMe_3[b]	$[Mo(CO)_3Cp]_2$
heptane	80	10	10
toluene	95	5	0
THF	100	0	0
$Mo(PR_3)_2(CO)_3$/tol[c]	0	0	100

[a] Mo = $Mo(CO)_2Cp$. [b] Mp = $Mo(CO)_3Cp$. [c] R = ^iPr, Cy; ^iPr = $CH(CH_3)_2$; Cy = C_6H_{11}.

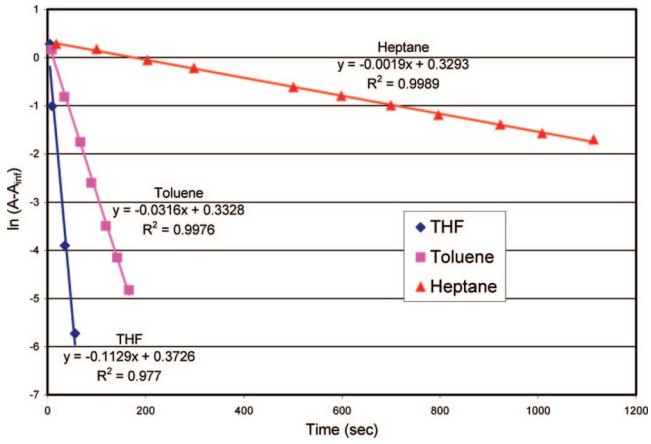

Figure 1. First-order plots of $\ln(A - A_\infty)$ versus time for the reaction of $HMo(CO)_3Cp$ (0.01 M) with $N_2CHSiMe_3$ (0.056 M) in heptane, toluene, and THF at 0 °C.

hydride and is readily followed by quantitative FTIR spectroscopic studies.[13] The product distribution of the reaction of HMp with $N_2CHSiMe_3$ was found to mainly depend on the solvent in which the reaction was carried out. This relationship between product distribution and solvent is shown in Table 1.

The reaction of $HMo(CO)_3Cp$ with $N_2CHSiMe_3$ was found to be first order in metal complex in all three solvents studied. Under pseudo-first-order conditions[14] with excess $N_2CHSiMe_3$ the rates were also seen to have a solvent dependence as shown in Figure 1. The plots of $\ln[A - A_\infty]$ versus time were linear through at least 2 half-lives.

The rate of reaction in toluene was roughly 16 times faster while the reaction in THF was observed to be approximately 57 times faster than the measured rate in heptane. As shown in Table 1, the reaction also produces more diazo complex as product on going from heptane to toluene to THF. No significant perturbation of the reaction rate was observed when the reaction was performed under an atmosphere of CO (as opposed to an atmosphere of Ar). The expected first-order dependence on $N_2CHSiMe_3$ was confirmed in heptane solution, where pseudo-first-order reactions at different $[N_2CHSiMe_3]$ (0.056 and 0.385 M) yielded the same derived rate constants within ~10% experimental error. The rates of reaction of HMp and DMp in heptane were also found to be the same within experimental error. As discussed later, this is attributed to H/D exchange between DMp and the diazoalkane. The rates of reaction of $HMo(CO)_3Cp^*$ ($Cp^* = \eta^5$-$C_5(CH_3)_5$) and $HW(CO)_3Cp$ were found to be slower than the reaction of $HMo(CO)_3Cp$. Derived rate constants for eq 9 are summarized in Table 2.

Table 2. Rate Constants for Reaction of Metal Hydrides and (Trimethylsilyl)diazomethane[a]

HML_n	T (°C)	solvent	k (M^{-1} s^{-1})
$HMo(CO)_3Cp$	0	heptane	0.035 ± 0.002
$HMo(CO)_3Cp$	0	toluene	0.56 ± 0.02
$HMo(CO)_3Cp$	0	THF	2.0 ± 0.3
$HMo(CO)_3Cp$	13	heptane	0.085 ± 0.005
$DMo(CO)_3Cp$	13	heptane	0.082 ± 0.005
$HMo(CO)_3Cp$	28	heptane	0.29 ± 0.01
$HMo(CO)_3Cp^*$	28	heptane	0.011 ± 0.001
$HW(CO)_3Cp$	28	heptane	0.0039 ± 0.0002

[a] Reactions were performed under pseudo-first-order conditions with $N_2CHSiMe_3$ in excess and obey the rate law $-d[HML_n]/dt = k[HML_n][N_2CHSiMe_3]$. First-order dependence on the metal- hydride complex was found for all data. First-order dependence in $N_2CHSiMe_3$ was confirmed for $HMo(CO)_3Cp$ in heptane only; other metal hydride data are for comparative purposes.

$$HMp + N_2CHSiMe_3 \rightarrow Mo(CO)_2(N_2CHSiMe_3)Cp + CO \quad (9)$$

An Eyring plot of the data in heptane solution is shown in the Supporting Information (Figure SF-1; $\Delta H^\ddagger = 11.7 \pm 2$ kcal/mol and $\Delta S^\ddagger = -22.0 \pm 3$ cal/(mol K)).

Reaction of $DMo(CO)_3Cp$ with $N_2CHSiMe_3$. Attempts were made to probe the kinetic isotope effect by investigating reactions of $HMo(CO)_3Cp$ and $DMo(CO)_3Cp$ (85 ± 10% isotopic enrichment) under comparable conditions. As shown in Figure SF-2 in the Supporting Information, these data yielded virtually identical rates and appeared to show no kinetic isotope effect within experimental error. The negligible value of the kinetic isotope effect $k(H)/k(D) = 1.04 \pm 0.05$ prompted NMR investigations of the reaction to see if H/D exchange occurred as shown in eq 10.

$$D{-}Mo(CO)_3Cp + N{=}N{=}CHSiMe_3 \rightleftharpoons H{-}Mo(CO)_3Cp + N{=}N{=}CDSiMe_3 \quad (10)$$

In the limiting case that H/D exchange was slow compared to the rate of eq 9, the use of D−Mp with 85% labeling would produce the $Mo(N_2CHDSiMe_3)$ complex in the ratio of 85:15 (HD:HH). That is, the product distribution would be independent of the presence of excess $N_2CHSiMe_3$ and, conversely, solely dependent upon the extent to which the H−Mp was isotopically labeled as D−Mp. However, if the H/D exchange is extremely rapid compared to the rate of eq 9, then full randomization of H/D would be expected. This would result in a statistical mixture of products as shown in eq 11.

$$D{-}Mo(CO)_3Cp + N_2CHSiMe_3(\text{excess}) \rightarrow N_2CDSiMe_3 + Mo(CO)_2CH_2SiMe_3 + Mo(CO)_2CHDSiMe_3 + Mo(CO)_2CD_2SiMe_3 \quad (11)$$

Control experiments showed that, once formed, the diazo complex did not undergo exchange with $DMo(CO)_3Cp$. Experiments were performed in heptane at 286 K by the addition of varying ratios of $N_2CHSiMe_3$ to $DMo(CO)_3Cp$, allowing the reaction to go to completion and then evacuating the reaction

(13) Products were identified qualitatively and quantitatively by FTIR bands as assigned in Table ST-1 in the Supporting Information and verified by comparison to authentic samples of recrystallized Mp_2 and Me_3SiCH_2Mp (independently prepared by the reaction of $NaMo(CO)_3Cp$ and $ClCH_2SiMe_3$). Peak positions assigned to the diazo compounds are in agreement with those originally reported by Lappert and Poland.[8]

(14) The pseudo-first-order conditions were typically in the range of a 5.7−10-fold excess of $N_2CHSiMe_3$, and the average concentration during the run was utilized. For a 5.75-fold excess, during 2 half lives the final $N_2CHSiMe_3$ will drop to 5.0. The average of 5.38 will thus vary by ~0.38/5.38 ≈ 7% during the course of the run. Somewhat surprisingly, this did not show up as a systematic deviation in fitting data to a straight line in $\ln[A - A_\infty]$ versus time plots in comparison to reactions in which a 10-fold excess of ligand was used. The lower amounts were used to slow down the reaction and also conserve the amount of diazoalkane used.

solution to dryness.[15] Samples were then redissolved in C_6D_6 and analyzed by ^1H NMR and FTIR spectroscopy. As shown in Figure SF-3 in the Supporting Information, the (H,H):(H,D):(D,D) product ratios were found to depend upon the relative concentrations of the reagents, implying that exchange as shown in eq 10 was in fact competitive with the overall reaction itself. More detailed analyses of these data (including both kinetic and equilibrium isotope effects)[16] was not attempted beyond the mechanistic observation of H/D exchange being more rapid than the overall reaction.

Spectroscopic Detection of an Intermediate Complex in Heptane Solution. Typical spectroscopic data for the overall reaction in heptane solution are shown in Figure SF-4 in the Supporting Information. These data show a smooth decay in the bands assigned to $HMo(CO)_3Cp$ and concomitant buildup of bands of the major product $Mo(CO)_2(N_2CH_2SiMe_3)Cp$, as well as the minor products $Mo(CO)_3(CH_2SiMe_3)Cp$ and $[Mo(CO)_3Cp]_2$. Expansion of the spectroscopic data during reaction in heptane at low temperature reveals bands at 2017 and 1930 cm^{-1} assigned to an intermediate complex (see Figure SF-5 in the Supporting Information). Following a rise time during the first spectrum, the bands near 2017 and 1930 cm^{-1} reach a maximum and then decay during the course of the reaction. A plot of the absorbance at 2017 cm^{-1} for the intermediate versus 2030 cm^{-1} for $HMo(CO)_3Cp$ showed reasonable linear behavior over the course of the reaction, as shown in Figure SF-6 in the Supporting Information. At higher concentrations of $N_2CHSiMe_3$ the bands assigned to the intermediate were observed to increase. These data are in keeping with formation of a preequilibrium complex between $N_2CHSiMe_3$ and HMp which goes on to products as shown in eq 12.

$$HMp + N_2CHSiMe_3 \underset{k_2}{\overset{k_1}{\rightleftharpoons}} \text{"I"} \rightarrow \text{Products} \qquad (12)$$

As discussed later, the intermediate, "I", is formulated as $[Me_3SiCH_2{-}N_\beta{=}N_\alpha{}^{\delta+}][{}^{\delta-}Mo(CO)_3Cp]$.

Thermodynamics of Reaction of $N_2CHSiMe_3$ with $HMo(CO)_3Cp$. The enthalpy of eq 9 was measured in THF by solution calorimetry at −1 °C. The resultant value of −9.5 ± 1.1 kcal/mol based on solid $HMo(CO)_3Cp$ yields a value with all species in solution of −11.6 ± 1.2 kcal/mol. Estimated data in toluene solution were found to be in agreement with this value.

Structure of $W(CO)_2(N_2CH_2SiMe_3)Cp$. The structure of $W(CO)_2(N_2CH_3)Cp$ has been reported by Hillhouse and Herrmann.[17] Determination of the structure of the analogous trimethylsilyl-substituted derivative was of interest to see if any significant differences occurred which might be indicative of bond strength differences. Within experimental error there are no significant differences. Crystals of this complex were grown by slow recrystallization from heptane, and the structure is shown in Figure 2 (full structural data are available as Supporting Information). The W−N1−N2 angle of 174.3° and the N1−N2−C8 angle of 117.4° are consistent with sp and sp^2 hybridizations on N1 and N2, respectively, and are consistent with the formulation $W{=}N{=}NCH_2SiMe_3$.

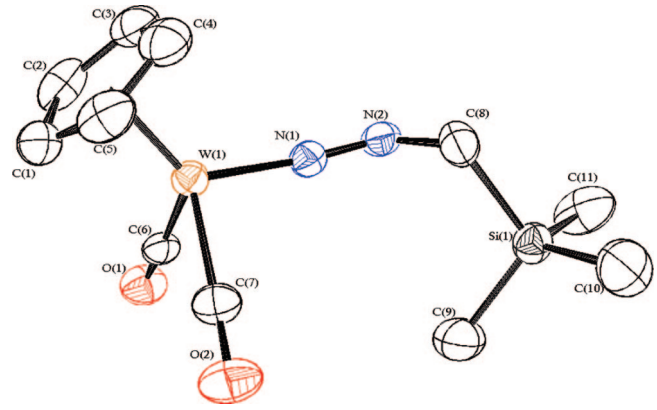

Figure 2. ORTEP drawing of $W(CO)_2(N_2CH_2SiMe_3)Cp$. Selected bond distances (Å) and angles (deg): W−N1 = 1.862(4), N1−N2 = 1.207(6), N2−C8 = 1.471(7), C8−Si1 = 1.898(6); W1−N1−N2 = 174.3(4), N1−N2−C8 = 117.4(5), N2−C8−Si = 110.6(4).

Reaction of 2 $HMo(CO)_3Cp$ with $N_2CHSiMe_3$ in the Presence of $M(PR_3)_2(CO)_3$ (M = Mo, W; R = Cy, ^{i}Pr): Catalytic Hydrogenation to $SiMe_4$ and $[Mo(CO)_3Cp]_2$. Coordination of $N_2CHSiMe_3$ to $M(PR_3)_2(CO)_3$ (M = Mo, W; R = Cy, ^{i}Pr) was investigated. $N_2CHSiMe_3$ was found[18] to be a better donor ligand than dinitrogen in terms of the equilibrium shown in eq 13.

$$(N_2)Mo(PR_3)_2(CO)_3 + N{=}NCHSiMe_3 \rightleftharpoons (Me_3SiHC{=}N{=}N)Mo(PR_3)_2(CO)_3 + N_2 \qquad (13)$$

The relatively strong binding of $N_2CHSiMe_3$ to this complex prompted an investigation of how this would alter the nature of reactivity of $N_2CHSiMe_3$ with $HMo(CO)_3Cp$. Surprisingly, the reaction occurred rapidly according to eq 14

$$(Me_3SiHCN_2)Mo(PR_3)_2(CO)_3 + 2HMp \rightarrow (N_2)Mo(PR_3)_2(CO)_3 + Mp_2 + SiMe_4 \qquad (14)$$

In stoichiometric reactions, the dinitrogen complex is observed as the final product of reaction 14. However, since this is readily displaced by the stronger ligand $N_2CHSiMe_3$, as shown in eq 13, reactions in which excess $N_2CHSiMe_3$ and HMp are combined in the presence of trace amounts of $M(PR_3)_2(CO)_3$ yield the catalytic hydrogen transfer reaction shown in eq 15. Such catalysis was also observed for other coordinatively

$$N_2CHSiMe_3 + 2\,HMp \xrightarrow{(N_2)Mo(P^iPr_3)_2(CO)_3} Mp_2 + SiMe_4 + N_2 \qquad (15)$$

unsaturated complexes of formula $M(PR_3)_2(CO)_3$ (M = Mo,W; R = Cy, ^{i}Pr).

(15) (a) The complex $Mo(CO)_2(N_2CH_2SiMe_3)Cp$ shows a singlet at 2.92 ppm, and the complex $Mo(CO)_2(N_2C(H)(D)SiMe_3)Cp$ shows a broad unresolved triplet at 2.90 ppm (in C_6D_6). However, analysis of these data required evacuation, which leads to some side products. Since $N_2CHSiMe_3$ was added in hexane and the reaction done in heptane, NMR analysis required evacuation to dryness and redissolution in C_6D_6. During concentration some decomposition was observed to occur, particularly for $Mo(CO)_3(CH_2SiMe_3)Cp$. The alkyl product can react further with $HMo(CO)_3Cp$.[31] (b) Jones, W. D.; Bergman, R. G. *J. Am. Chem. Soc* **1979**, *101*, 5447.

(16) Bullock, R. M. In *Transition Metal Hydrides*; Dedieu, A., Ed.; VCH: New York, 1991; p 263.

(17) Hillhouse, G. L.; Haymore, B. L.; Herrmann, W. A. *Inorg. Chem.* **1979**, *18*, 2423.

(18) The enthalpies of this and related reactions have been measured and will be reported separately: Fortman, G. C.; Isrow, D.; McDonough, J. E.; Weir, J. J.; Kubas, G. J.; Scott, B.; Hoff, C. D. Manuscript in preparation.

Scheme 1. Computed Energies (B3LYP/6-311+G) Relevant to the Thermochemical Cycle for Hydrogenation of $N_2CHSiMe_3$[a]**

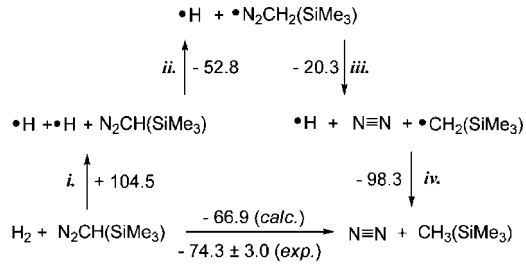

[a] All values in kcal/mol.

Enthalpy of Hydrogenation of $N_2CHSiMe_3$. The reaction shown in eq 15 provided a means to determine the enthalpy of formation of $N_2CHSiMe_3$. This is possible due to the fact that the enthalpy of eq 16 has previously been reported.

$$Mp_2 + H_2 \rightarrow HMp \quad \Delta H = +6.3 \pm 1.0 \text{ kcal/mol} \quad (16)$$

Pure $HMo(CO)_3Cp$ was used as the limiting reagent in the solution calorimetric studies. The selective nature of the catalysis by $M(P^iPr_3)_2(CO)_3$ (M = Mo, W) was verified, in that quantitative conversion to only Mp_2 and $SiMe_4$ was observed. Production of these products was confirmed by NMR spectroscopy. Values for the enthalpy of reaction were independent of whether the Mo or W analogue was used as a catalyst. Adding the measured enthalpy of the reaction shown in eq 15) -80.6 ± 2.0 kcal/mol, to the reaction in eq 16 yields the enthalpy of the reaction in eq 17 to be equal to -74.3 ± 3.0 kcal/mol.

$$N_2CHSiMe_3(soln) + H_2(gas) \rightarrow SiMe_4(soln) + N_2(gas) \quad (17)$$

The enthalpies of mixing of both $N_2CHSiMe_3$ and $SiMe_4$ in toluene are expected to be less than 1 kcal/mol and largely cancel. The enthalpy of formation of $N_2CHSiMe_3$ is calculated as 5.8 ± 3.0 kcal/mol, on the basis of the standard enthalpy of formation of $SiMe_4$ of -68.5 kcal/mol.[19]

Computed Enthalpy of Hydrogenation of $N_2CHSiMe_3$. The experimental value for ΔH of eq 17 in the solution phase (-74.3 ± 3.0 kcal/mol) can be compared to the computational result of -67 kcal/mol derived from B3LYP/6-311+G** in the gas phase, as shown in Scheme 1 above. Step i in this scheme is simple dissociation of H_2, and step ii is addition of •H to N=N=C(H)$SiMe_3$ to yield •N=NR, where R = CH_2SiMe_3. Step iii is a key step, since it shows that dissociation of •CH_2SiMe_3 from •N=NCH_2SiMe_3 is considerably more exothermic than that computed for loss of •H from •N=NH, for which values of -3.8 and -8 kcal/mol have been reported.[20]

Computed Structure and Bond Strengths of $M(CO)_2(N_2CH_2SiMe_3)Cp$ (M = Mo, W). Computed structures for $M(CO)_2(N_2CH_2SiMe_3)Cp$ (M = Mo, W) at the BP86 level are shown in Figure 3.

The theoretical bond lengths for the W complex are in good agreement with the actual structure shown in Figure 2. The computed geometries of $Mo(CO)_2(N_2CH_2SiMe_3)Cp$ and $W(CO)_2(N_2CH_2SiMe_3)Cp$ are very similar. Conversely, the charge distribution shows a notable difference between them, as molybdenum carries a negative charge and tungsten carries a partial positive charge in the analogous complexes. Accordingly, NBO analysis reveals some difference in the metal−nitrogen bond polarization: the bond is 56% polarized toward nitrogen in $Mo(CO)_2(N_2CH_2SiMe_3)Cp$ and 59% polarized toward nitrogen in $W(CO)_2(N_2CH_2SiMe_3)Cp$. The largest contributions in the metal−nitrogen NBOs involve the valence d_{xz} natural atomic orbitals (NAOs) of the transition metals and the $2p_z$ NAOs of nitrogen. The Wiberg bond indices are 1.295 for $Mo(CO)_2(N_2CH_2SiMe_3)Cp$ and 1.325 for $W(CO)_2(N_2CH_2SiMe_3)Cp$.

The M−$N_2CHSiMe_3$ bond dissociation enthalpy according to eq 18 was calculated to be 74.3 kcal/mol (M = Mo) and 83.3 kcal/mol (M = W).

$$M(CO)_2(N_2CH_2SiMe_3)Cp \rightarrow {}^{\bullet}M(CO)_2Cp + {}^{\bullet}N_2CH_2SiMe_3 \quad (18)$$

This compares to that computed for loss of CO as shown in eq 19.

$$^{\bullet}M(CO)_3Cp \rightarrow {}^{\bullet}M(CO)_2Cp + CO \quad (19)$$

The enthalpy of eq 19 is computed to be 52.0 kcal/mol for M = Mo and 59.8 kcal/mol for M = W. The computed absolute bond strength data seem somewhat higher than expected, on the basis of the OC−$M(CO)_5$ bond strengths, which are 40 and 46 kcal/mol for Mo and W, respectively.[21] Of direct relevance to this work is the difference between eqs 19 and 18:

$$^{\bullet}M(CO)_3Cp + {}^{\bullet}N_2CH_2SiMe_3 \rightarrow M(CO)_2(N_2CH_2SiMe_3)Cp + CO \quad (20)$$

The computed enthalpies of eq 20 are -22.3 kcal/mol for M = Mo and -23.5 kcal/mol for M = W and reflect the computed bond strength differences between CO and the diazo group. The computed difference for Mo of -22.3 kcal/mol is in good agreement with an independent analysis based on experimental data of -25 ± 5 kcal/mol, as discussed later. Thus, while the individual Mo−CO and Mo−$N_2CHSiMe_3$ bond strengths may be somewhat higher than experimental data, the difference between the two ligands is relatively close.

Computed Structure and Homolytic Bond Cleavage of $HM(CO)_3Cp$ Complexes. Computation of potential reaction pathways of $HM(CO)_3Cp$ and $N_2CHSiMe_3$ required initial calculation of the structure and energy of the hydrides themselves. Surprisingly, two minima were found for $HM(CO)_3Cp$ potential energy hypersurfaces for Mo and W and are shown in Figure SF-7 of the Supporting Information. The lowest energy structures (**MoH-e** and **WH-e**) have the hydrido ligand in an equatorial position. This structure corresponds closely to the neutron diffraction structure[22] reported for H−$Mo(CO)_3Cp^*$ and is taken as the ground state. A second (local) minimum was found in which the hydrido ligand was located in an axial position directly opposite and below the C_5H_5 ring system (**MoH-a** and **WH-a**). **MoH-a** and **WH-a** possessed a free energy ~7.8 (Mo) and 9.7 (W) kcal/mol above the ground-state configuration. We are not aware of computations of this second structural pattern. The transition state connecting the two minima has a low barrier, and fluxional behavior of this relatively "soft" potential energy surface would be expected.

(19) (a) Steele, W. V. *J. Chem. Thermodyn.* **1983**, *15*, 595. (b) Davalos, J. Z.; Baer, T. *J. Phys. Chem. A* **2006**, *110*, 8572. (c) http://webbook.nist.gov.

(20) A computed value of 3.8 kcal/mol for addition of •H to N2 (a) Gu, J.; Xie, Y.; Schaefer, H. F. *J. Chem. Phys.* **1998**, *108*, 8029. A computed value of 8 kcal/mol for addition of •H to N_2: (b) Matus, M. H.; Arduengo, A. J.; Dixon, D. A. *J. Phys. Chem.* **2006**, *110*, 10116.

(21) Smith, G. P. *Polyhedron* **1988**, *7*, 1605.

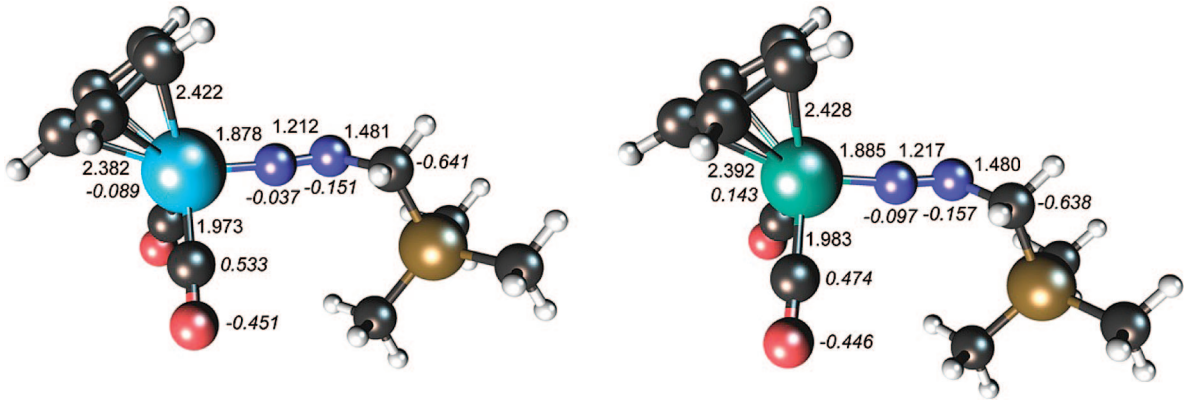

Figure 3. Computed structure of $Mo(CO)_2(N_2CH_2SiMe_3)Cp$ (left) and $W(CO)_2(N_2CH_2SiMe_3)Cp$ (right). Bond lengths are given in angstrom; natural charges are given in italics.

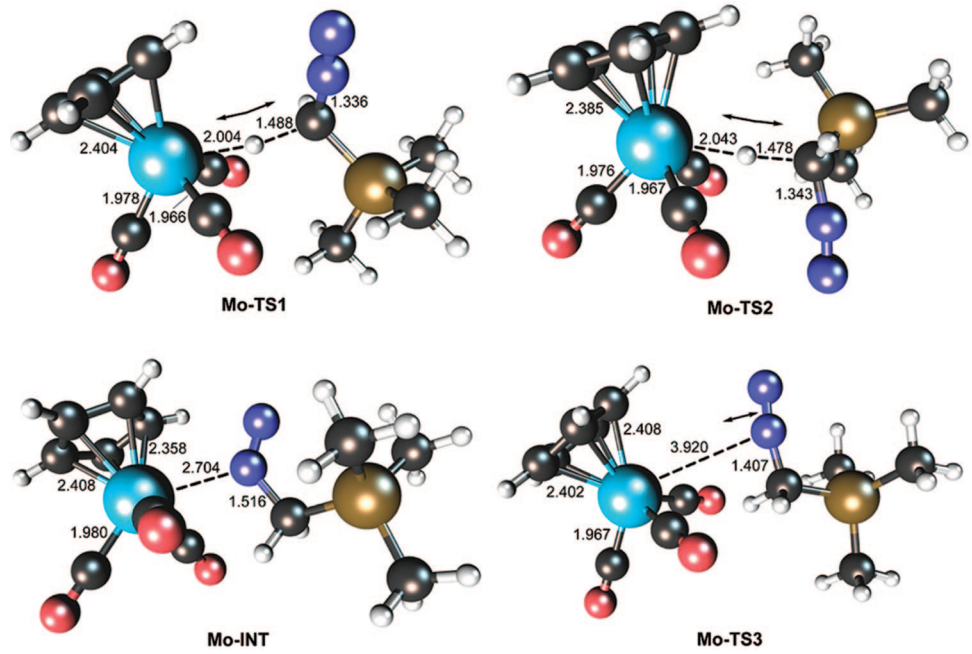

Figure 4. Structures of possible transition states describing the proton transfer and of the intermediate containing a loose Mo−N bond (values given in Å).

The charge distributions show minor differences in the cases of the two metals, and molybdenum is found to be more negative than tungsten, as in the earlier complexes. The results of the harmonic vibrational frequency analyses are in reasonable agreement with the available experimental data, seen in Table ST-2 of the Supporting Information. The strengths of the metal−hydrogen bonds in the four minima were also examined, and the results are summarized in Table ST-3 of the Supporting Information. The differences in Wiberg bond indices are consistent with the enthalpies and free energies associated with the bond dissociation.

Computed Intermediates and Transition States in the Reaction of HMo(CO)Cp with $N_2CHSiMe_3$. The seminal isomer involved in the initial proton transfer process from the hydrido complex to (trimethylsilyl)diazomethane, which is discussed later, is the **MoH-e** isomer shown in Figure SF-7. The **MoH-e** isomer is calculated to be the global minimum. Computed structures on the reaction pathway are shown in Figure 4. Two slightly different orientations of the diazoalkane (**Mo-TS1** and **Mo-TS2**), which are shown in Figure 4, were observed in the reaction leading to **Mo-INT**. The structure of **Mo-INT** is proposed to be a polar coordinate bond capable of dissociation to the ion pair $[Mo(CO)_3Cp]^-[N_2CH_2SiMe_3]^+$. The lowest energy pathway going from **MoH-e** to the proposed intermediate **Mo-INT** through **Mo-TS1** was calculated to possess a barrier of 17.5 kcal/mol. Proton transfer through the transition state **Mo-TS2** possessed a barrier of 19.9 kcal/mol.

The structure of **Mo-TS3** in Figure 4 corresponds to the transition state for dissociation of this ion pair. Computed solvated energies using the PCM method are summarized in Table 3. The computed energies of dissociation to ion pairs of 25.8, 25.2, and 23.6 kcal/mol in heptane, toluene, and THF are in qualitative agreement with experimental observations. For heptane solution at 298 K a value of $\Delta G^{\ddagger} = 18.3 \pm 5.0$ kcal/mol (from experimental data $\Delta H^{\ddagger} = 11.7 \pm 2.0$ kcal/mol and $\Delta S^{\ddagger} = -22.0 \pm 3.0$ cal/(mol K)) was calculated. While the experimental value is 7.5 kcal/mol lower than the computed value, the agreement is within the errors expected for calculations (and experiment) on such difficult systems. The ratio of rates based on computed solvent activation parameters gives closer agreement: the computed relative rates at 298 K are ca. 1:3:40, compared to experimental values at 273 K of ca. 1:16:57 for heptane, toluene, and THF, respectively. The computa-

Table 3. Computed Gibbs Free Energies and Gibbs Free Energies of Activation (kcal/mol) for Reaction of $HMo(CO)_3Cp$ with $N_2CHSiMe_3$ as a Function of Solvent[a]

phase	$\Delta G_1°$ [b]	$\Delta G^‡$ [c]	$\Delta G_2^‡$ [d]	$\Delta G° + \Delta G_2^‡$ [e]
gas phase	15.7	17.5	10.9	26.6
heptane	16.4	17.9	9.4	25.8
toluene	16.5	19.9	8.7	25.2
THF	17.1	18.2	6.5	23.6

[a] Solvated free energies computed using the PCM method. [b] Refers to the $\Delta G°$ value for the reaction of $HMo(CO)_3Cp$ and $N_2CHSiMe_3$ to give **Mo-INT** of Figure 4. [c] Refers to the $\Delta G^‡$ value for the reaction $HMo(CO)_3Cp$ and $N_2CHSiMe_3$ to give **Mo-INT** through **Mo-TS1**. [d] Refers to the $\Delta G^‡$ value for **Mo-TS3** through **Mo-INT** of Figure4. [e] Total computed free energy to the transition state for dissociation to ion pairs.

tions provide a model for the transition state, and the computed data are in reasonable accord with experiment.

Discussion

One goal of this work was to determine the thermochemical barriers to N_2 insertion, as shown in eq 8, comparable to those already reported for CO insertion, as shown in eq 7. In addition, we sought to compare the bonding capabilities of NO and N_2R as ligands. For N_2 insertion to be favorable, a strong bond between the metal and the N_2R fragment is required. As discussed earlier, unlike OCR or NO, the N_2R fragment itself is unstable. A blend of theory and experiment is required to analyze the bonding. In order to start investigations in this area, we initially sought conditions to achieve a clean reaction of $HMo(CO)_3Cp$ with $N_2CHSiMe_3$ to yield a single product.

Proposed Mechanism for Reaction of $HMo(CO)_3Cp$ and $N_2CHSiMe_3$. The lack of an inhibiting influence of CO on the rate of reaction discounted steps involving ligand displacement of carbon monoxide by a diazo group. However, it does suggest either H atom transfer, as shown in eq 21, or proton transfer, as shown in eq 22, as the initial step of the reaction.

$$HM(CO)_3Cp + N_2CHSiMe_3 \rightarrow {}^{\bullet}M(CO)_3Cp + {}^{\bullet}N_2CH_2SiMe_3 \quad (21)$$

$$HM(CO)_3Cp + N_2CHSiMe_3 \rightarrow [M(CO)_3Cp]^-[N_2CH_2SiMe_3]^+ \quad (22)$$

Theoretical calculations discussed earlier showed that the C−H bond strength formed in ${}^{\bullet}N_2CH_2SiMe_3$ (+53 kcal/mol) is weaker than the bond broken in H−$Mo(CO)_3Cp$ (+66 kcal/mol) by ∼13 kcal/mol. The experimentally observed enthalpy of activation of +11.7 ± 2 kcal/mol is lower than this value but overlaps within experimental error. Therefore, eq 21 cannot be ruled out.

Key findings were that the H/D exchange was faster than the overall reaction itself and that both the rate and product distribution were solvent dependent. A plausible mechanism consistent with all observations discussed in the Results is shown in Scheme 2. The first step in Scheme 2 involves formation of an initial adduct by rapid proton transfer from the metal hydride to the carbene carbon[23] and formation of the proposed key intermediate complex. The intermediate can be viewed either as a tight ion pair or as an η^1-diazo complex bonded to N_β, as shown in Scheme 2. The reversible nature of the protonation/deprotonation step accounts for the H/D scrambling that is observed. The computed structure of this intermediate is shown in Figure 4 as **Mo-INT**; rapid H/D exchange could presumably occur from either of the two transition states shown. Separation of the ion pair and recombination at N_α would result in formation of the diazo complex, which is the major reaction product. This corresponds roughly to the reaction shown in eq 1, but in which the arene diazonium salt is replaced with the alkyl diazonium cation formed by protonation of (trimethylsilyl)diazomethane. Following migration from N_β to N_α, loss of CO yields the final product in which the ${}^{\bullet}N_2CH_2SiMe_3$ is now a formal three-electron-donor ligand.

The increased tendency to dissociate to ion pairs as more coordinating solvents are used is in keeping with the fact that on going from heptane to toluene to THF the reaction becomes both faster and shows fewer side products.

The products of diazoalkane protonations have long been postulated to depend on the rate of escape from the solvent cage of initial ion pairs formed. In studies of the reactions in alcohol of diazoalkanes with benzoic acid, the product ratio has been interpreted in terms of the relative rates of escape of the ions from the initial ion pair, with ester product arising from a tight ion pair and ether product from escape.[24] This ratio was found to not be temperature dependent but to depend critically on solvent polarity. The role of cage effects in photochemical reactions of $[W(CO)_3Cp]_2$ and PR_3 ligands has been recently studied.[25]

Retention of the initial ion pair (favored in more nonpolar solvents), however, could result in electron transfer to yield radical products, as shown in eq 23.

$$[M(CO)_3Cp]^-[N_2CH_2SiMe_3]^+ \rightarrow {}^{\bullet}M(CO)_3Cp + {}^{\bullet}N_2CH_2SiMe_3 \quad (23)$$

This corresponds to the net reaction for H atom transfer and is kinetically indistinguishable from eq 21 occurring directly. The fact that the computed activation energy for eq 21 is only marginally higher than the observed activation energy supports the close balance between these two processes. Computational results suggest that formation of a free ${}^{\bullet}N_2CH_2SiMe_3$ radical would be expected to result in rapid expulsion of N_2, as shown in eq 24.

$${}^{\bullet}N_2CH_2SiMe_3 \rightarrow {}^{\bullet}CH_2SiMe_3 + N_2 \quad (24)$$

The radicals ${}^{\bullet}CH_2SiMe_3$ and ${}^{\bullet}Mo(CO)_3Cp$ would then be free to form the alkyl product if they combine directly. Reaction of ${}^{\bullet}CH_2SiMe_3$ and $HMo(CO)_3Cp$ in solution would be expected[26] to rapidly form $SiMe_4$ and ${}^{\bullet}Mo(CO)_3Cp$. Combination of two ${}^{\bullet}Mo(CO)_3Cp$ radicals will rapidly form $[Mo(CO)_3Cp]_2$. The solvent dependence on reaction products as well as spectroscopic detection of an intermediate appears to be in accord with these observations.

The mechanism in Scheme 2 is proposed to involve a polar addition of H^+ in a reversible first step. This might be expected to depend on the pK_a of the metal hydride. In comparison to $HMo(CO)_3Cp$ (pK_a = 6.4; H_2O), $HMo(CO)_3Cp^*$ (pK_a = 9.6; H_2O) and $HW(CO)_3Cp$ (pK_a = 8.6; H_2O) are both weaker

(22) Brammer, L.; Zhao, D.; Bullock, R. M.; McMullan, R. K. *Inorg. Chem.* **1993**, *32*, 4819.

(23) Zollinger, H. *Diazo Chemistry*; VCH: New York, 1995; Vol. 2, p 303

(24) (a) Baer, T.; Bauer, S. H. *J. Am. Chem. Soc.* **1970**, *92*, 4773. (b) More O'Ferrall, R. A.; Kwok, W. K.; Miller, S. I. *J. Am. Chem. Soc.* **1964**, *86*, 24–5553.

(25) Cahoon, J. F.; Kling, M. F.; Schmatz, S.; Harris, C. B. *J. Am. Chem. Soc.* **2005**, *127*, 12555.

(26) Franz, J. A.; Linehan, J. C.; Birnbaum, J. C.; Hicks, K. W.; Alnajjar, M. S. *J. Am. Chem. Soc.* **1999**, *121*, 9824.

Scheme 2. Proposed Mechanism for the Reaction of HMo(CO)Cp with $N_2CHSiMe_3$, Producing Diazo, Alkyl, and Metal−Metal Dimer Products

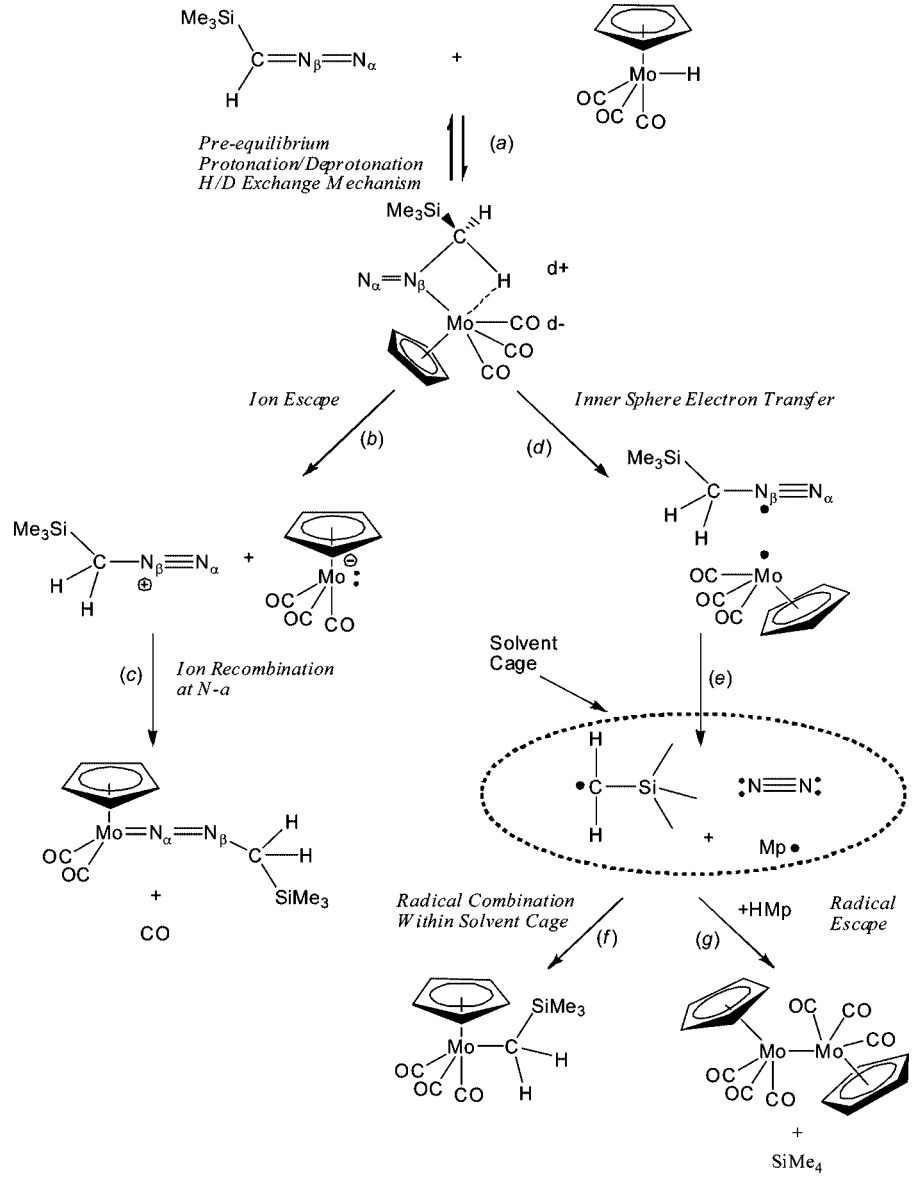

acids.[27] Investigations of these two other hydrides showed that they reacted more slowly. At $T = 28$ °C $HMo(CO)_3Cp^*$ was found to react approximately 26 times more slowly and $HW(CO)_3Cp$ approximately 75 times more slowly than $HMo(CO)_3Cp$. It is worth noting that in reactions of $HMo(CO)_3Cp^*$ both alkyl and metal−metal dimer side products are formed, as was the case for $HMo(CO)_3Cp$. However, reactions of $HW(CO)_3Cp$ with $N_2CHSiMe_3$ in heptane produced exclusively $W(CO)_3(CH_2SiMe_3)Cp$ as a side product. $[W(CO)_3Cp]_2$ was not produced in any detectable amount.

Reaction of $HMo(CO)_3Cp$ with $N_2CHSiMe_3$ in the Presence of $Mo(P^iPr_3)_2(CO)_3$, M = Mo, W). The reaction of $Mo(CO)_3Cp$ with $N_2CHSiMe_3$ was observed to be much more rapid in the presence of $M(P^iPr_3)_2(CO)_3$, in spite of the new steric barriers presented by the $M(P^iPr_3)_2(CO)_3$ fragment surrounding the $N_2CHSiMe_3$. The observed increased rate of reaction may be due to the coordination of the $N_2CHSiMe_3$ to the electron-rich metal center which in turn could shift the proposed initial protonation/deprotonation of the diazo group, as shown in eq 25. The increased basicity of coordinated

$$(Me_3SiHCN_2)Mo(P^iPr_3)_2(CO)_3 + HMo(CO)_3Cp \rightleftharpoons [(Me_3SiH_2CN_2)Mo(P^iPr_3)_2(CO)_3]^+ + [Mo(CO)_3Cp]^- \quad (25)$$

diazoalkanes has been reported by Eisenberg.[28] The strong π basicity of $Mo(P^iPr_3)_2(CO)_3$ has been demonstrated by Kaim and co-workers,[29] where the methylpyrazine cation was found to form a stable complex. Thus, it is plausible that the methyldiazonium cation would remain bound to the complex $Mo(P^iPr_3)_2(CO)_3$ and that this protonation/deprotonation equilibrium is, first, rapidly established and, second, more favorable for the bound diazo relative to the free group.

(27) Kristjansdottir, S. S.; Norton, J. R. In *Transition Metal Hydrides*; Dedieu, A., Ed., VCH: New York, 1991; p 322.

(28) Woodcock, C.; Eisenberg, R. *Organometallics* **1985**, *4*, 4.

(29) (a) Bruns, W.; Hausen, H. D.; Kaim, W.; Schulz, A. *J. Organomet. Chem.* **1993**, *444*, 121. (b) Bruns, W.; Kaim, W.; Waldhoer, E.; Krejcik, M. *Inorg. Chem.* **1995**, *34*, 663.

Scheme 3. Proposed Steps in the Catalytic Hydrogenation of $N_2CHSiMe_3$ by $HMo(CO)_3Cp$ in the Presence of $Mo(CO)_3(P^iPr_3)_2$[a]

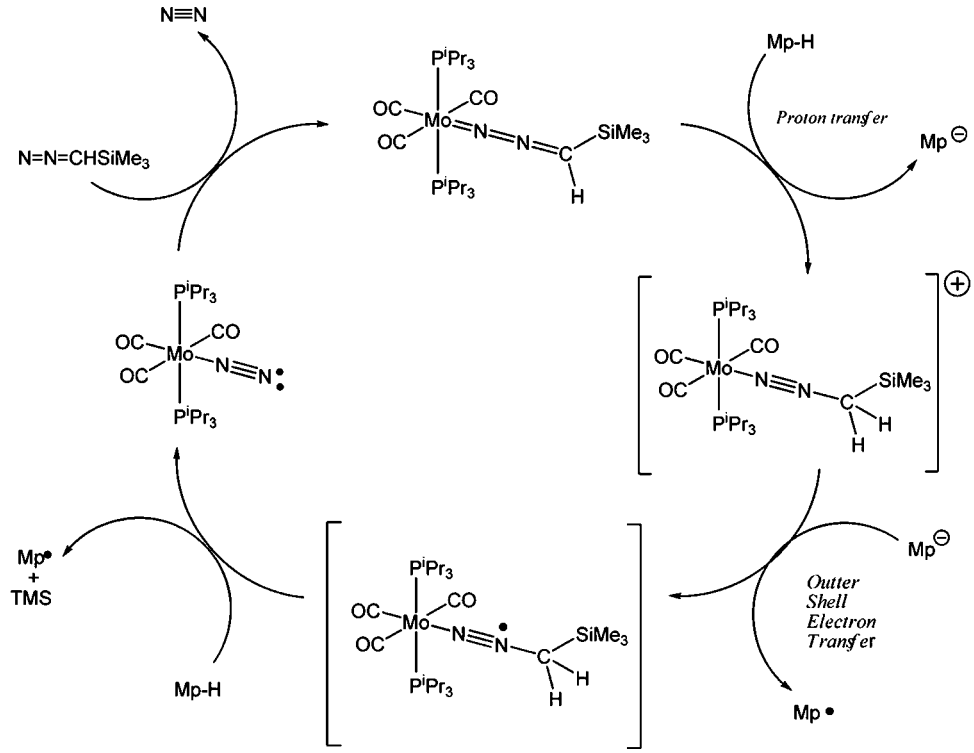

[a] A step not shown is combination of 2 $^{\bullet}Mo(CO)_3Cp$ radical to yield $[Mo(CO)_3Cp]_2$ (Mp = $Mo(CO)_3Cp$).

Scheme 4. Thermochemical Cycle Used To Calculate the Enthalpy of the Homolytic Bond Formation between $^{\bullet}Mo(CO)_3Cp$ and $^{\bullet}N_2CHSiMe_3$[a]

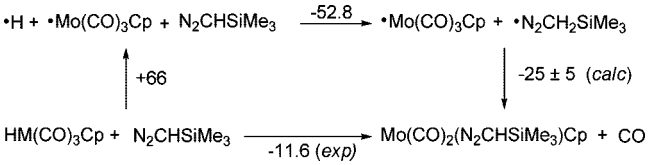

[a] All values are in kcal/mol.

Scheme 5. Thermochemical Cycle Used To Estimate the Enthalpy of Insertion of Molecular Nitrogen into the Mo−R Bond of $Mo(CO)_3(CH_3)Cp$[a]

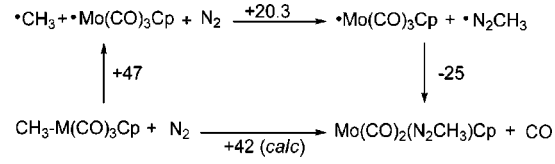

[a] All values are in kcal/mol.

Due to the steric factors, the reaction channel involving migration from N_β to N_α which leads to the diazo complex as shown in Scheme 2 would be blocked when the diazoalkane is coordinated. A plausible proposed mechanism for the catalytic process is summarized in Scheme 3.

Thermochemistry of the Formation of $Mo(CO)_2(N_2CH_2SiMe_3)Cp$. Data generated in this work was used to estimate the enthalpy of eq 26 to be -25 ± 5 kcal/mol.

$$^{\bullet}Mo(CO)_3Cp + {}^{\bullet}N_2CH_2SiMe_3 \rightarrow Mo(CO)_2(N_2CH_2SiMe_3)Cp + CO \quad (26)$$

This value was calculated using the thermochemical cycle shown in Scheme 4. The combination of the Mo−H bond strength in $HMo(CO)_3Cp$ of 66 kcal/mol[30] and the enthalpy of $^{\bullet}H$ addition to $N_2CHSiMe_3$ of -52.8 kcal/mol (computed as shown in Scheme 1) with the experimental net enthalpy of reaction of -11.6 kcal/mol allowed for the estimation of the enthalpy of displacement of CO by the diazenido radical fragment. This value overlaps within experimental error the independently computed difference between the Mo−CO and Mo−$NNCHSiMe_3$ bonds of 22.3 kcal/mol discussed earlier.

This can also be compared to data for eq 2 ($\Delta H = -33.2 \pm 1.8$ kcal/mol), where the $^{\bullet}N{=}O$ radical displaces CO in the corresponding $^{\bullet}Cr(CO)_3Cp^*$ radical. There is a larger gap in energy between $^{\bullet}N{=}O$ and CO for Cr than between $^{\bullet}N_2CH_2SiMe_3$ and CO for Mo. Work is in progress to expand data in this series to allow more accurate assessment of bond strength trends in these and related complexes.

The data generated here can be further used to estimate the energy required for N_2 insertion into the Mo−R bond for R−$Mo(CO)_3Cp$, as shown in eq 8. In spite of the strong Mo−diazo bond formed, the insertion is predicted to be uphill by $\sim 42 \pm 5$ kcal/mol, as shown in Scheme 5. This estimate was made using the H_3C−Mo BDE of 47 kcal/mol in $Mo(CO)_3(CH_3)Cp$[31] and the computed endothermic addition of an alkyl radical to N_2 of 20 kcal/mol as shown in Scheme 1, together with the value of -25 ± 5 kcal/mol estimated from Scheme 4 for the enthalpy of displacement of CO by $^{\bullet}N_2CH_2SiMe_3$.

(30) Landrum, J. T.; Hoff, C. D. *J. Organomet. Chem.* **1985**, *282*, 215.

(31) Nolan, S. P.; Lopez de la Vega, R.; Mukerjee, S. L.; Gonzalez, A. A.; Zhang, K.; Hoff, C. D. *Polyhedron* **1988**, *7*, 1491.

This suggests that prior photochemical loss of CO from R−Mo(CO)$_3$Cp would result in a nearly thermoneutral reaction, since the Mo−CO bond is ∼40 kcal/mol. In this regard, nitrile insertion has been recently reported[32] to occur in the photochemical/thermal reaction sequence shown in eq 27. This

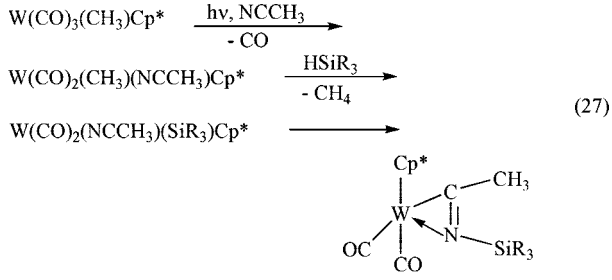

(27)

observed N≡CR insertion in this photochemically generated nitrile complex provides hope that the goal of analogous photochemical N≡N insertion may not be out of reach. In the case of N_2 insertion, the final product would presumably be an η^1-diazo complex rather than the η^2 binding motif observed for the nitrile product in eq 27.

Enthalpy of Formation of $N_2CH_2SiMe_3$. The catalytic hydrogenation of $N_2CHSiMe_3$ by HMo(CO)$_3$Cp outlined in Scheme 3 allowed reasonably accurate determination of the enthalpy of formation of this reactive diazo compound in solution to be 5.8 ± 3.0 kcal/mol. Key aspects of this measurement were that the determination relied on the purified organometallic reagent HMo(CO)$_3$Cp and that the catalysis by Mo(P^{i}Pr$_3$)$_2$(CO)$_3$ cleanly led to the products $SiMe_4$ and [Mo(CO)$_3$Cp]$_2$. This line of approach, in which an organic compound too reactive to be isolated in neat form can be addressed by its reaction with organometallic reagents of known thermochemistry which are easier to purify and characterize thermochemically, may find an increased use in the future.

Experimental Section

General Procedures. Unless stated otherwise, all operations were performed in a Vacuum Atmospheres glovebox under an atmosphere of purified argon or utilizing standard Schlenk tube techniques under argon. THF, toluene, and heptane were purified by distillation under argon from sodium benzophenone ketyl into flame-dried glassware and then degassed. Solutions of (trimethylsilyl)diazomethane in hexanes (2.0 M) were purchased from Aldrich and used without further purification. HMo(CO)$_3$Cp,[33] HW(CO)$_3$Cp,[33] HMo(CO)$_3$Cp*,[34] and M(PR$_3$)$_2$(CO)$_3$ (M = Mo, W; R = ^{i}Pr, Cy)[35] were prepared by standard literary procedures. The metal hydrides were further purified by sublimation at ca. 60 °C and 10^{-2} Torr. The complexes M(CO)$_2$N$_2$CH$_2$SiMe$_3$Cp (M = Mo, W) were characterized by FTIR, NMR, and mass spectroscopy, as well as X-ray crystallography for M = W. FTIR and NMR data were found to be in agreement with those originally reported by Lappert and Poland.[8] A sample of Me$_3$SiCH$_2$Mo(CO)$_3$Cp was prepared by reaction of NaMo(CO)$_3$Cp and ClCH$_2$SiMe$_3$ and shown to have spectroscopic properties identical with those detected in solution-phase studies. FTIR data were obtained on a Perkin-Elmer System 2000 spectrometer fitted with a microscope and flow-through cell that has been described in detail elsewhere.[36] NMR spectra were obtained on a Bruker AVANCE 400 MHz spectrometer. MS spectra were obtained on a VG MASSLAB TRIO-2 instrument using FAB techniques.

Kinetic Studies of the Reaction of HM(CO)$_3$Cp with $N_2CHSiMe_3$. In a typical procedure, a solution of 0.1 g of HMo(CO)$_3$Cp in 35 mL of heptane was prepared in a Schlenk tube under argon to make a 0.0012 M solution. The solution was then loaded into a syringe in the glovebox. A Hamilton gastight syringe fitted with a valve was filled with 1.00 mL of a 2.0 M solution of $N_2CHSiMe_3$ in hexanes. Both syringes were taken from the glovebox. The hydride solution was transferred under an argon atmosphere to a 50 mL thermostated glass reactor with a magnetic stir rod. The system was connected to a Schlenk line and also to the Perkin-Elmer 2000 FTIR microscope system by means of a small-diameter Teflon tube. Following temperature equilibration approximately 1 mL of the hydride solution was transferred under argon to the FTIR cell and a stock solution spectrum recorded. The reaction was started by injection of the $N_2CHSiMe_3$ solution, and periodically small samples were removed for analysis by transfer to the flow-through cell. Similar procedures under a CO atmosphere were performed with careful ventilation.

NMR Studies of H/D Exchange. In the glovebox a Schlenk tube was charged with 0.2057 g of DMo(CO)$_3$Cp, which was then dissolved in 25.0 mL of heptane (0.035 M) under argon. One milliliter of this solution was used for taking an FTIR spectrum, and to three different Schlenk tubes was added 8.0 mL of this solution. These tubes were removed from the glovebox and connected to a Schlenk line. All three Schlenk tubes were placed in an ice bath at 0 °C. After temperature equilibration 1.0 mL of a 2.0 M solution of $N_2CHSiMe_3$ in hexanes was added to one of the tubes. To the other two tubes 0.100 and 0.025 mL of the diazo solution were added, respectively. All three flasks were allowed to stand for 1 h at 0 °C. At that time the reaction was judged to be complete by FTIR spectra, and all volatile material was removed from each flask by vacuum. C_6D_6 (3.0 mL) was added to the solid residue in each flask, and the material dissolved with no trace of residual solids. Each solution was analyzed by FTIR and ^{1}H NMR spectroscopy. In addition to the expected major product Mo(CO)$_2$(N$_2$CH$_x$D$_{2-x}$SiMe$_3$)Cp, FTIR bands showed both the known [Mo(CO)$_3$Cp]$_2$ and Me$_3$SiCH$_2$Mo(CO)$_3$Cp and unidentified minor additional products. These unidentified products were attributed to reactions that most likely occurred upon concentration during the evacuation of the sample and were judged to not significantly influence the NMR analysis of the major products (Mo(CO)$_2$(N$_2$CH$_x$D$_{2-x}$SiMe$_3$)Cp).

Crystal Growth and Structure of W(CO)$_2$N$_2$CH$_2$SiMe$_3$Cp. Crystals of W(CO)$_2$(N$_2$CH$_2$SiMe$_3$)Cp suitable for structure determination were prepared by dissolving 0.1002 g of HW(CO)$_3$Cp in 10 mL of toluene (0.0030 M). To this solution was added 0.200 mL of a 2.0 M $N_2CHSiMe_3$ solution in hexanes. After the addition of $N_2CHSiMe_3$ the solution turned from a clear orange to a dark red. The reaction was allowed to continue for a period of approximately 80 min, and the product was characterized by FTIR spectroscopy. The major product of the reaction was W(CO)$_2$(N$_2$CH$_2$SiMe$_3$)Cp. A side reaction also led to the formation of W(CO)$_3$(CH$_2$SiMe$_3$)Cp. Peak assignments for these compounds can be seen in Table ST-1 in the Supporting Information. The solution was then evaporated to dryness and the residue redissolved in 4.0 mL of heptane. A portion of the W(CO)$_2$(N$_2$CH$_2$SiMe$_3$)Cp remained undissolved. The solution was removed and filtered into a glass tube under argon. The remaining undissolved portion was dissolved in another 4.0 mL of heptane and used to characterize the product by IR spectroscopy. The glass tube was sealed under

(32) Suzuki, E.; Komuro, T.; Okazaki, M.; Tobita, H. *Organometallics* **2007**, *26*, 4379.
(33) King, R. B. *Organometallic Synthesis*; Academic Press: New York, 1961; Vol. 1, p 165.
(34) Kubas, G. J.; Kiss, G.; Hoff, C. D. *Organometallics* **1991**, *10*, 2870.
(35) Wasserman, H. J.; Kubas, G. J.; Ryan, R. R. *J. Am. Chem. Soc.* **1986**, *108*, 2294.
(36) Ju, T. D.; Capps, K. B.; Roper, G. C.; Hoff, C. D. *Inorg. Chim. Acta* **1998**, *270*, 488.

vacuum and placed in a freezer (~−20 °C) for a period of 2 weeks. The tube was opened in the glovebox; the mother liquor was removed by syringe and replaced with a small amount of degassed mineral oil. The tube was then sealed again and stored until mounting for structure determination.

Crystal Structure Determination. Due to air sensitivity the crystal was mounted from a pool of mineral oil under an argon gas flow. The crystal was placed on a Bruker P4 diffractometer with 1k CCD and cooled to 203 K using a Bruker LT-2 temperature device. The instrument was equipped with a sealed, graphite-monochromated Mo Kα X-ray source (λ = 0.710 73 Å). A hemisphere of data was collected using φ scans, with 30 s frame exposures and 0.3° frame widths. Data collection and initial indexing and cell refinement were handled using SMART[37] software. Frame integration, including Lorentz−polarization corrections, and final cell parameter calculations were carried out using SAINT[38] software. The data were corrected for absorption using the SADABS[39] program. The decay of reflection intensity was monitored via analysis of redundant frames. The structure was solved using direct methods and difference Fourier techniques. All hydrogen atom positions were idealized and rode on the atom they were attached to. The final refinement included anisotropic temperature factors on all non-hydrogen atoms. Structure solution, refinement, graphics, and creation of publication materials were performed using SHELXTL.[40]

Reaction of $HM(CO)_3Cp$ with $N_2CH_2SiMe_3$ in the Presence of $M(PR_3)_2(CO)_3$ Complexes (M = Mo, W; R = ^{i}Pr$_3$, Cy). In the glovebox 0.2044 g of solid $Mo(PCy_3)_2(CO)_3$ (0.27 mmol) was dissolved in 10.0 mL of toluene to which 0.2 mL of a 2.0 M solution of $N_2CHSiMe_3$ in hexanes (0.4 mmol) was added. An FTIR spectrum was run and showed peaks at 2066 cm^{-1} due to free $N_2CHSiMe_3$ (~0.13 mmol) as well as bands at 1948 (w), 1844 (s), 1833 (sh) cm^{-1} assigned to $Mo(PCy_3)_2(CO)_3(N_2CHSiMe_3)$ (~0.27 mmol). In addition, a small band at 1866 cm^{-1} was present, due to the known and unreactive complex $Mo(PCy_3)_2(CO)_4$, which is a common contaminant of the air-sensitive $Mo(PCy_3)_2(CO)_3$. In a second Schlenk tube a solution of freshly sublimed $HMo(CO)_3Cp$ (0.0811 g 0.33 mmol) was prepared in 10 mL of toluene and then added to the solution of $Mo(PCy_3)_2(CO)_3(N_2CHSiMe_3)$. An FTIR spectrum run within minutes of mixing showed new bands attributed to $[Mo(CO)_3Cp]_2$. No bands due to $HMo(CO)_3Cp$, $Mo(CO)_2(N_2CH_2SiMe_3)Cp$, or free $N_2CHSiMe_3$ were seen. The FTIR data for $Mo(PCy_3)_2(CO)_3(N_2CHSiMe_3)$ was largely unchanged. Bands assigned to the known complexes $Mo(PCy_3)_2(CO)_3$ and $Mo(PCy_3)_2(CO)_3(N_2)$ were present, in keeping with the calculated stoichiometry of the reaction: 2 HMp (0.33 mmol) + $Mo(PCy_3)_2(CO)_3(N_2CHSiMe_3)$ (0.27 mmol) + $N_2CHSiMe_3$ (0.13 mmol) → Mp_2 (0.165 mmol) + $Mo(PCy_3)_2(CO)_3(N_2CHSiMe_3)$ (0.235 mmol) + $Mo(PCy_3)_2(CO)_3(N_2)$/$Mo(PCy_3)_2(CO)_3$ (0.035 mmol) + N_2 (0.165 mmol) + $SiMe_4$ (0.165 mmol). In separate experiments performed in C_6D_6 the production of $SiMe_4$ was proven by NMR spectroscopy. Addition of CO to the reaction mixture described above showed IR bands attributable to free $N_2CHSiMe_3$ generated from $Mo(PCy_3)_2(CO)_3(N_2CHSiMe_3)$ as well as conversion of all other products except Mp_2 and $Mo(PCy_3)_2(CO)_4$.

Repetition of this reaction at room temperature with varying ratios of reagents showed that both $Mo(PCy_3)_2(CO)_3$ and $Mo(P^iPr_3)_2(CO)_3$ as well as the corresponding W derivatives produced clean hydrogenation of $N_2CHSiMe_3$ from HMp in toluene, even at 4/1 ratios of free $N_2CHSiMe_3$ to bound $N_2CHSiMe_3$. No detectable amount of $Mo(CO)_2(N_2CH_2SiMe_3)Cp$ was observed in the room-temperature reactions.

Calorimetric Measurement of the Enthalpy of Reaction of $HMo(CO)_3Cp$ with $N_2CH_2SiMe_3$ in THF. In the glovebox a solution of 350 mL of THF and 10 mL of 2.0 M $N_2CHSiMe_3$ in hexanes was prepared in a Schlenk flask. The solution was transferred to the calorimeter. Also in the glovebox a glass ampule was filled with 0.2204 g of $HMo(CO)_3Cp$ (0.90 mmol). The ampule was sealed under vacuum and was then placed inside the calorimeter and allowed to come to thermal equilibrium at 272 K under stirring.

Upon equilibration the calorimeter was electrically calibrated by heating a standardized resistor with a known current for typically 60 s. The system was then allowed to reestablish thermal equilibrium over a period of (on average) 15−20 min. The reaction was then initiated, and the thermogram was recorded electronically at 10 s intervals. The calorimeter was once again left to reach thermal equilibrium. Once equilibrium was reached, the calorimeter was electrically calibrated. The average of the two electrical calibrations was used to evaluate the heat given off in the reaction. Six total runs were averaged together to obtain a final value of −9.5 ± 1.1 kcal/mol. Correction for the endothermic enthalpy of solution of solid $HMo(CO)_3Cp$ (+2.1 ± 0.1 kcal/mol in THF) yielded a final value with all species in THF solution of −11.6 ± 1.2 kcal/mol.

After all runs were completed, the final products of the several runs of calorimetry were verified by FTIR spectroscopy. The main peaks at the end of the experiment were assigned to excess $N_2CHSiMe_3$ (2065 cm^{-1}) and the final product of $Mo(CO)_2(N_2CH_2SiMe_3)Cp$. Trace amounts of $Mo(CO)_2(CH_2SiMe_3)$ were also seen in the spectrum. Both products' peak assignments can be seen in Table ST-1 of the Supporting Information. Also, small peaks at 1862 and 1804 cm^{-1} were seen and are believed to be due to unknown decomposition products.

Calorimetric Measurement of the Enthalpy of Hydrogenation of $N_2CH_2SiMe_3$ by $HMo(CO)_3Cp$ in the Presence of $W(CO)_3(P^iPr_3)_2N_2CHSiMe_3$. In the glovebox a solution of 10.0 mL of toluene and 0.400 mL of 2.0 M $N_2CHSiMe_3$ in hexane was prepared. To this solution was added 0.2080 g of $W(CO)_3(P^iPr_3)_2$ (0.36 mmol). One milliliter of this solution was used for recording an FTIR spectrum, and 4 mL was loaded under argon into the cell of a Setaram-C-80 Calvet microcalorimeter. The solid-containing compartment of the calorimeter was loaded with 0.0206 g of freshly sublimed $HMo(CO)_3Cp$. The assembled calorimeter cell was taken from the glovebox and loaded into the calorimeter. After the system reached temperature equilibration, the reaction was initiated and the thermogram indicated a rapid reaction which returned cleanly to baseline with no thermal signal indicative of any substantial secondary reactions occurring.

Following a return to the baseline, the cell was taken back into the glovebox, and a sample analyzed by FTIR spectroscopy showed the presence of $W(CO)_3(P^iPr_3)_2(N_2CHSiMe_3)$, $N_2CHSiMe_3$, $[Mo(CO)_3Cp]_2$, and $W(CO)_4(P^iPr_3)_2$ the last of which is present whenever handling $W(CO)_3(P^iPr_3)_2$. The spectral peaks of these compounds are given in Table ST-1 of the Supporting Information. The reported enthalpy of reaction is the average of five measurements and yielded an average value based on solid $HMo(CO)_3Cp$ of −37.2 ± 0.9 kcal/mol. Correction for the endothermic enthalpy of solution of solid $HMo(CO)_3Cp$ (+3.1 ± 0.1 kcal/mol in toluene) yielded a final value with all species in toluene solution of −40.3 ± 1.0 kcal/mol of reacting $HMo(CO)_3Cp$ −80.6 ± 2.0 kcal/mol of $N_2CHSiMe_3$ reacting. The derived enthalpy of reaction was found to be the same when $Mo(CO)_3(P^iPr_3)_2(N_2CHSiMe_3)$ was used in place of $W(CO)_3(P^iPr_3)_2(N_2CHSiMe_3)$ as catalyst for the hydrogenation.

Computational Details. Full geometry optimizations have been performed at the density functional level of theory without any symmetry constraints using the Gaussian 03 suite of programs.[41]

(37) SMART-NT 4; Bruker AXS, Inc., Madison, WI 53719, 1996.
(38) SAINT-NT 5.050; Bruker AXS, Inc., Madison, WI 53719, 1998.
(39) Sheldrick, G. SADABS, first release; University of Göttingen, Göttingen, Germany.
(40) SHELXTL Version 6.10; Bruker AXS, Inc., Madison, WI 53719; 2001.
(41) Frisch, M. J. Gaussian 03, Revision B.05; Gaussian, Inc., Pittsburgh, PA, 2003.

For all of the calculations the gradient-corrected exchange functional developed by Becke[42] was utilized in combination with a correlation functional developed by Perdew[43] and denoted as BP86. For molybdenum and tungsten the valence triple-ζ SDD basis set following the (8s7p6d1f) → [6s5p3d1f] contraction pattern is utilized with the corresponding relativistic effective core potential.[44] For the other atoms the 6-311G(d,p) basis set was used.[45] The density fitting basis sets were generated automatically from the AO primitives by the Gaussian 03 program. The stationary points were characterized by frequency calculations in order to verify that they have zero imaginary frequencies for equilibrium geometries and one imaginary frequency for transition states. The NBO analyses were carried out on the stationary points using the NBO 3.1 program[46] as implemented in Gaussian. To estimate the effect of the solvent, single-point calculations on the gas-phase optimized structures were carried out using the polarized continuum model (PCM)[47] with the dielectric constant values $\epsilon_0 = 1.92$, 2.38, 7.58 for heptane, toluene, and tetrahydrofuran, respectively. Thermochemistry corrections were taken from gas-phase frequency calculations at 298.15 K and 1 atm.

Acknowledgment. We dedicate this article to Professor R. Bruce King of the University of Georgia and thank Professor Joel Liebman, the University of Maryland, Baltimore County, and Dr. Manuel Temprado for helpful discussions. Support of this work by the National Science Foundation (Grant Nos. CHE 0615743 and CHE 0716718) and by the Hungarian Scientific Research Fund (Grant No. OTKA NK 71906) is gratefully acknowledged.

Supporting Information Available: Tables and figures giving experimental and computed vibrational spectroscopic data, computed minimum energies of $HM(CO)_3Cp$ for M = Mo, W, and kinetic and spectroscopic data and a CIF file giving crystallographic data for the structure of $W(CO)_2(N_2CH_2SiMe_3)C_5H_5$. This material is available free of charge via the Internet at http://pubs.acs.org.

OM800336P

(42) Becke, A. D. *Phys. Rev. A* **1988**, *38*, 3098.
(43) Perdew, J. P. *Phys. Rev. B* **1986**, *33*, 8822.
(44) Dolg, M.; Stoll, H.; Preuss, H.; Pitzer, R. M. *J. Phys. Chem.* **1993**, *97*, 5852.
(45) Krishnan, R.; Binkley, J. S.; Seeger, R.; Pople, J. A. *J. Chem. Phys.* **1980**, *72*, 650.
(46) Glendening, E. D.; Reed, A. E.; Carpenter, J. E.; Weinhold, F. NBO Version 3.1.
(47) Miertus, S.; Scrocco, E.; Tomasi, J. *Chem. Phys.* **1981**, *55*, 117.